

# Ion-beam nanotexturing of buffer layers for near-single-crystal thin-film deposition: Application to $\text{YBa}_2\text{Cu}_3\text{O}_{7-\delta}$ superconducting films

R. P. Reade, P. Berdahl, and R. E. Russo

*Environmental Energy Technologies Division, Lawrence Berkeley National Laboratory, Berkeley, California 94720*

(Received 31 July 2001; accepted for publication 6 December 2001)

A method of producing biaxially textured template layers for near-single-crystal-quality film growth on substrates that do not provide a template for oriented crystalline growth is described and compared to existing methods. This technique, ion-beam nano texturing (ITEX), produces a biaxially textured layer by oblique ion irradiation of an amorphous film surface. Using *in situ* reflection high-energy electron diffraction and *ex situ* x-ray diffraction, an yttria-stabilized zirconia (YSZ) template layer fabricated by ITEX is shown to have the appropriate surface texture for  $\text{YBa}_2\text{Cu}_3\text{O}_{7-\delta}$  coated conductor fabrication. A  $\text{YBa}_2\text{Cu}_3\text{O}_{7-\delta}$  thin film deposited on an ITEX YSZ layer has a critical current of  $2.5 \times 10^5 \text{ A/cm}^2$  (77 K,  $1 \mu\text{V/cm}$ ). ITEX produces texture rapidly and should be ideally suited for future low-cost manufacturing. © 2002 American Institute of Physics.

[DOI: 10.1063/1.1450059]

There has recently been an increasing interest in the deposition of near-single-crystal quality thin films on substrates that do not provide a template for epitaxial crystalline growth. These substrates include many technically important materials such as randomly oriented polycrystalline metal foils, amorphous insulators such as  $\text{SiO}_2$ , and plastics. A primary example is the desire to deposit the high-temperature superconductor  $\text{YBa}_2\text{Cu}_3\text{O}_{7-\delta}$  (YBCO) on a flexible Ni-based superalloy [such as Haynes Alloy No. 230 (HA230)] to make high-current conductors in the form of tapes. To carry high currents (critical current density  $J_c > 10^6 \text{ A/cm}^2$  at 77 K), the YBCO material must be near-single-crystal quality, as critical current decreases with increasing grain boundary angles in the film.<sup>1,2</sup> Flexible polycrystalline metal substrates do not provide the proper template for such growth.

Three approaches have been used to promote oriented YBCO crystalline growth on substrates that do not provide an epitaxial template. One approach, initially demonstrated by Sumitomo using yttria-stabilized zirconia (YSZ),<sup>3</sup> produces texture by depositing a buffer layer with a vapor source at an inclined angle. Recent results for similarly deposited MgO buffer layers have demonstrated good texture, with a YBCO  $\phi$  scan full-width-half-maximum (FWHM)  $\sim 9^\circ$  and  $J_c \sim 7.9 \times 10^5 \text{ A/cm}^2$ .<sup>4</sup> The textured layers are tilted toward the axis of the vapor source ( $\sim 25^\circ$ ). This results in asymmetric in-plane  $J_c$ s in YBCO layers grown on these buffers. Thick ( $> 1 \mu\text{m}$ ) MgO layers are required to achieve suitable texture for YBCO deposition.

A second approach for fabricating YBCO superconductor tapes utilizes metallographic rolling and thermal annealing to induce texture directly in a Ni metal foil.<sup>5</sup> This method is promising, with YBCO  $\phi$  scan FWHM  $\sim 7^\circ$  and  $J_c$ s over  $10^6 \text{ A/cm}^2$  demonstrated in tapes. Oxidation of the Ni surface during deposition and problems transferring the epitaxial template to the YBCO film have thus far only been overcome by a multilayer buffer structure, such as  $\text{CeO}_2/\text{YSZ}/\text{CeO}_2$ . This additional processing may increase manufacturing costs. Also, this technique limits the choice of substrates to a few metals.

A third approach for fabricating high-current YBCO tapes on flexible metal foil (as well as other structures including YBCO/amorphous insulator multilayers<sup>6</sup>) is ion-beam assisted deposition (IBAD) of a textured template layer, pioneered by Iijima *et al.*<sup>7</sup> and Reade *et al.*<sup>8</sup> in 1992. The IBAD process utilizes oblique angle ion bombardment during the deposition of a buffer layer, most commonly YSZ, to produce a biaxially aligned (both normal and in-plane axes aligned) template layer. This process can be used to make a template layer on almost any substrate, enabling a wide variety of near-single-crystal thin film applications on substrates that do not provide a template for epitaxial crystalline growth. Recent results using IBAD demonstrate that this process can be used to fabricate high-current YBCO tapes.<sup>9</sup> Our results as well as those of others<sup>10</sup> have shown that the texture of the IBAD YSZ buffer layer improves with thickness, and therefore deposition time. To produce the texture necessary for YBCO tapes ( $\phi$  scan FWHM  $< 10^\circ$ ), more than  $1.0 \mu\text{m}$  of YSZ film is needed. This result is consistent with the model of Bradley *et al.*, which predicts a gradual improvement in texture due to a competitive grain growth mechanism, followed by an asymptotic approach to a saturation value.<sup>11</sup> IBAD deposition rates are low (typically  $< 50 \text{ nm/min}$ ) due to the fact that ion flux to material flux ratios are critical during this process (increasing ion flux improves texture, but slows deposition due to sputtering). Therefore, IBAD YSZ deposition times of over 20 min are required for YBCO tapes, which is too slow for typical industrial processing.

Recent IBAD results using a process developed at Stanford<sup>12</sup> for MgO template layers have demonstrated biaxial texture in a much thinner layer ( $\sim 10 \text{ nm}$ ) than with YSZ. YBCO  $\phi$  scan FWHM  $\sim 11^\circ$  and  $J_c \sim 8.6 \times 10^5 \text{ A/cm}^2$  (75 K) have been reported using this process.<sup>13</sup> This process employs an amorphous layer of silicon nitride under the MgO, and substrate roughness effects have been reported to lower  $J_c$ s.

We now report a simpler and faster technique to produce a template for near-single-crystal films on difficult substrates—Ion-beam nano texturing (ITEX). ITEX uses



FIG. 1. (Color) RHEED image from YSZ surface after ITEX processing. There is some magnetic distortion evident due to the close proximity of the ion source.

ion-beam parameters similar to IBAD, but differs fundamentally in that the buffer layer deposition is separate from the texturing process. An amorphous layer of buffer material is first deposited by a rapid technique. This layer is then exposed to oblique ion irradiation to produce texture in the near-surface region of the film. This textured surface layer is then used as the template for near-single-crystal film growth. In cases when the desired substrate material is amorphous to begin with, ITEX can be applied directly to the substrate, eliminating the need for a buffer layer. ITEX is much faster and thus more industrially applicable than IBAD, as one can use an inexpensive and fast method to deposit the initial amorphous material, and then treat the surface rapidly with the ion beam.

To demonstrate the ITEX process, we fabricated a textured YBCO/YSZ/HA230 structure as follows. A mechani-

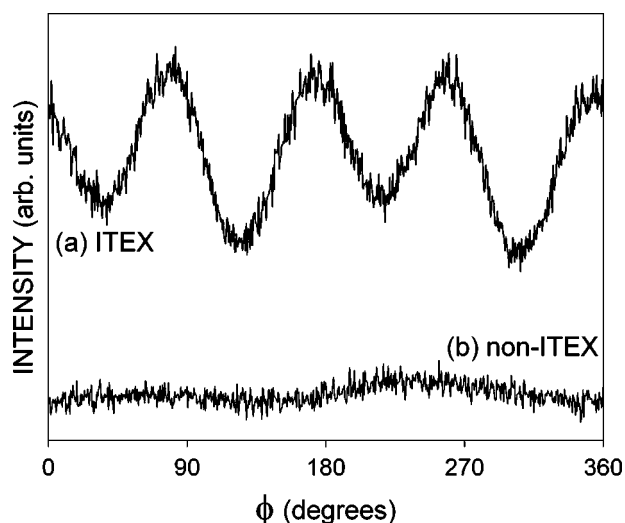


FIG. 2. (103) YBCO  $\phi$  scans from YBCO thin films on (a) ITEX YSZ and (b) non-ITEX amorphous YSZ.

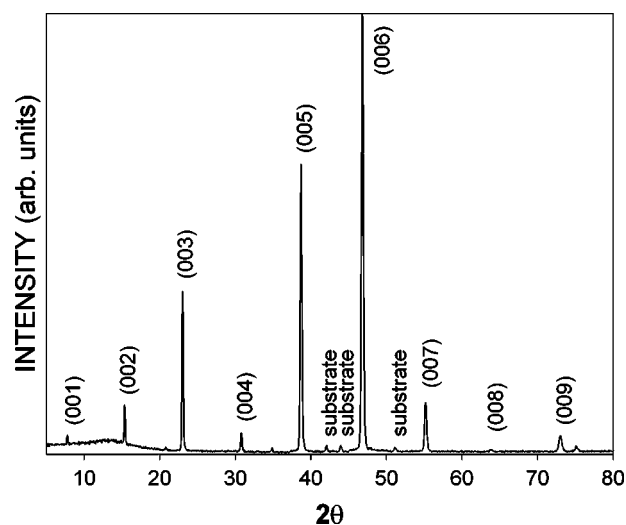


FIG. 3. XRD from YBCO/ITEX-YSZ/HA230 sample, showing strong (001) YBCO peaks.

cally polished ( $0.05\ \mu\text{m}$  alumina final polish) HA230 substrate was first coated with YSZ using pulsed-laser deposition (PLD) conditions previously shown to produce an amorphous layer (room temperature,  $<10^{-6}$  Torr vacuum).<sup>14</sup> This amorphous YSZ layer was then subjected to 300 eV  $\text{Ar}^+$  ion bombardment at  $\sim 55^\circ$  from the surface normal (the same as typically used for IBAD of YSZ) for 1.5 min. at a pressure of 0.8 mTorr (50%  $\text{Ar}$ , 50%  $\text{O}_2$ ). The penetration depth of oblique 300 eV  $\text{Ar}^+$  is expected to be about 1–2 nm,<sup>15,16</sup> so only a thin layer near the surface is likely to be directly modified. Finally, a YBCO thin film was deposited using our standard PLD process.<sup>14</sup> The simplicity of this processing sequence is notable, especially since the YSZ buffer deposition and the ITEX texturing are performed independently, avoiding the rate issues of IBAD.

A Staib Instruments differentially-pumped 35 keV *in situ* reflection high-energy electron diffraction (RHEED) system was used to generate an *in situ* image from the surface of the YSZ produced during ITEX processing (Fig. 1). The azimuth of the RHEED beam is perpendicular to the azimuth of the ion beam in this analysis. This diffraction pattern clearly shows that crystallinity is induced at the surface of the previously amorphous YSZ surface. The pattern shows that the incident electron beam is parallel to a (110) YSZ axis, as expected for a (001) YSZ surface. A rotation of the sample in the plane of the film shows a fourfold symmetry, with the expected (001) pattern  $45^\circ$  from the (110) axis, thus verify-

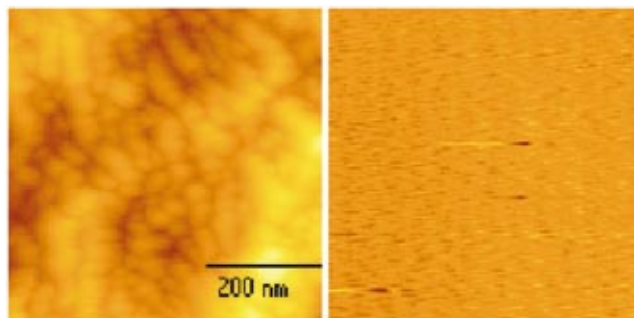


FIG. 4. (Color) AFM images of (a) ITEX and (b) non-ITEX amorphous YSZ surfaces.

ing that a (001) film surface has been created with biaxial texture in the plane of the film. These patterns are similar to those demonstrated for an IBAD YSZ surface.<sup>17</sup> There is some distortion in the pattern, due to the close proximity of the strong permanent magnets in the ion source. Modifications are being made to the system to increase the distance between the ion source and the substrate to eliminate this distortion.

A (103) YBCO  $\phi$  scan, shown in Fig. 2(a), demonstrates that in-plane texture was established in the YBCO film deposited on the ITEX YSZ. For comparison, a sample was made with an otherwise identical process but without ITEX—this sample did not exhibit in-plane texture in a  $\phi$  scan [Fig. 2(b)]. Though the ITEX texture is not as good as that produced by a well-optimized IBAD process,<sup>9</sup> this result is similar to early IBAD results.<sup>7,8</sup> The  $J_c$  measured on a 50  $\mu\text{m}$  bridge was  $2.5 \times 10^5 \text{ A/cm}^2$  (77 K, 1  $\mu\text{V/cm}$ ). The ITEX process has not yet been optimized; further work is underway to determine the effects of process parameters on the texture and resulting  $J_c$ .

To further establish that ITEX has produced a (001) textured YSZ surface, a Bragg–Bretano x-ray diffraction (XRD) pattern is shown in Fig. 3. It is apparent that the ITEX YSZ surface provided a suitable template for strong  $c$ -axis crystallization of the YBCO film. A pattern generated for the sample that was not textured by ITEX showed peak intensities that were less than 25% of those for the ITEX sample. Note that the broad hump in the XRD patterns at low  $2\theta$  angles indicates that the YSZ material is still largely amorphous beneath the textured surface.

An atomic force microscopy (AFM) image of the ITEX YSZ surface is shown in Fig. 4(a), with an image of an untreated amorphous YSZ surface in Fig. 4(b). The ITEX YSZ surface shows 20–40 nm features that do not appear on the untreated surface. These features can be attributed to crystallization of small YSZ grains on the surface, induced by the ITEX process.

The use of oblique angle ion texturing of a buffer-layer surface to form a biaxial template for subsequent crystalline thin film growth is new, although the fact that ion-beam irradiation can produce structural transformations in materials is well established. In particular, it is known that ion bombardment can cause the crystallization of amorphous materials;  $\text{SiO}_2$ <sup>18</sup> and carbon<sup>19</sup> are among the materials that have been crystallized by energetic beam irradiation. Also, it has been shown that the crystallites in polycrystalline metals can be realigned by ion bombardment.<sup>20</sup> The degree of biaxial orientation that ITEX can create during crystallization on an amorphous surface needs to be determined, but the RHEED pattern in Fig. 1 already appears similar to patterns obtained during IBAD processing. Ion energy is one critical parameter. High energy ions (keV) are known to cause amorphization of crystalline materials (including metals at low temperature), so there is an upper limit above which crystallization is not to be expected. Even at the high end of the allowable energy range, it is possible that the material sputtering rate could overwhelm the nanotexturing rate, removing textured material as quickly as it can be formed. At very low ion energies, the resulting defects may not be sufficient to enable crystallization. The effects of ion energy as

well as other parameters need further exploration to enhance the degree of texture beyond that demonstrated in this initial work.

For YSZ, the ITEX process may produce surface texture equal to or better than that produced by IBAD. Though the exact mechanisms of the process are still not understood, two main theories for IBAD texturing of materials like YSZ have been advanced. (It is important to note that a different mechanism has been proposed for IBAD of  $\text{MgO}$ .<sup>12</sup>) Bradley *et al.*<sup>11</sup> and others have proposed a competitive sputtering mechanism in which nonaligned grains in the growing film are limited in their growth due to a higher sputtering rate than for aligned grains. Ensinger<sup>16</sup> and Ressler *et al.*<sup>21</sup> argue that such a sputtering rate differential does not exist, but that the alignment occurs due to an anisotropic ion damage accumulation mechanism. In either case, however, it is a competitive grain growth process which eventually (after the deposition of an order of 1000 crystal unit cells) results in a highly textured surface. ITEX is a direct surface texturing process that does not rely on a competitive grain growth mechanism. Since this nanotexturing is a simpler process, it may be more readily understood and controlled.

The authors are grateful for the technical advice of Eugene Haller, John Clarke, and Mark Levine. This work was supported by the Lawrence Berkeley National Laboratory, Laboratory Directed Research and Development program, under Contract No. DE-AC03-76SF00098.

- <sup>1</sup>D. Dimos, P. Chaudhari, and J. Mannhart, *Phys. Rev. B* **41**, 4038 (1990).
- <sup>2</sup>Z. G. Ivanov, P. A. Nilsson, D. Winkler, J. A. Alarco, T. Claeson, E. A. Stepantsov, and A. Y. Tzalenchuk, *Appl. Phys. Lett.* **59**, 3030 (1991).
- <sup>3</sup>K. Hasegawa, H. Mukai, M. Konishi, J. Fujikami, K. Ohmatsu, K. Hayashi, K. Sato, S. Honjo, H. Ishii, Y. Sato, and Y. Iwata, in *Advances in Superconductivity X*, edited by K. Osamura and I. Hirabayashi (Springer, Tokyo, 1998), p. 607.
- <sup>4</sup>M. Bauer, R. Semerad, and H. Kinder, *IEEE Trans. Appl. Supercond.* **9**, 1502 (1999).
- <sup>5</sup>C. Park, D. P. Norton, D. K. Christen, D. T. Verebelyi, R. Feenstra, J. D. Budai, A. Goyal, D. F. Lee, E. D. Specht, D. M. Kroeger, and M. Paranthaman, *IEEE Trans. Appl. Supercond.* **9**, 2276 (1999).
- <sup>6</sup>R. P. Reade and R. E. Russo, *Appl. Surf. Sci.* **96–98**, 726 (1996).
- <sup>7</sup>Y. Iijima, N. Tanabe, O. Kohno, and Y. Ikeno, *Appl. Phys. Lett.* **60**, 769 (1992).
- <sup>8</sup>R. P. Reade, P. Berdahl, S. M. Garrison, and R. E. Russo, *Appl. Phys. Lett.* **61**, 2231 (1992).
- <sup>9</sup>S. R. Foltyn, P. N. Arendt, P. C. Dowden, R. F. DePaula, J. R. Groves, J. Y. Coulter, Q. X. Jia, M. P. Maley, and D. E. Peterson, *IEEE Trans. Appl. Supercond.* **9**, 1519 (1999).
- <sup>10</sup>M. P. Chudzik, R. Erck, M. T. Lanagan, and C. R. Kannewurf, *IEEE Trans. Appl. Supercond.* **9**, 1490 (1999).
- <sup>11</sup>R. M. Bradley, J. M. E. Harper, and D. A. Smith, *J. Appl. Phys.* **60**, 4161 (1986).
- <sup>12</sup>C. P. Wang, K. B. Do, M. R. Beasley, T. H. Geballe, and R. H. Hammond, *Appl. Phys. Lett.* **71**, 2955 (1997).
- <sup>13</sup>J. R. Groves, P. N. Arendt, H. Kung, S. R. Foltyn, R. F. DePaula, and L. A. Emmert, *IEEE Trans. Appl. Supercond.* **11**, 2822 (2001).
- <sup>14</sup>R. P. Reade, X. L. Mao, and R. E. Russo, *Appl. Phys. Lett.* **59**, 739 (1991).
- <sup>15</sup>V. A. Miteva and I. R. Chakarov, *Vacuum* **51**, 267 (1998).
- <sup>16</sup>W. Ensinger, *Nucl. Instrum. Methods Phys. Res. B* **106**, 142 (1995).
- <sup>17</sup>V. Betz, B. Holzapfel, and L. Schultz, *IEEE Trans. Appl. Supercond.* **7**, 1436 (1997).
- <sup>18</sup>T. Mizutani, *J. Non-Cryst. Solids* **181**, 123 (1995).
- <sup>19</sup>C. B. Lioutas, N. Vouroutzis, S. Logothetidis, and S. Bouladakis, *Carbon* **36**, 545 (1998).
- <sup>20</sup>D. Dobrev, *Thin Solid Films* **92**, 41 (1982).
- <sup>21</sup>K. G. Ressler, N. Sonnenberg, and M. J. Cima, *J. Am. Ceram. Soc.* **80**, 2637 (1997).